

# An Integrated Approach to Uncover Drivers of Cancer

Uri David Akavia,<sup>1,2,5</sup> Oren Litvin,<sup>1,2,5</sup> Jessica Kim,<sup>3,4</sup> Felix Sanchez-Garcia,<sup>1</sup> Dylan Kotliar,<sup>1</sup> Helen C. Causton,<sup>1</sup> Panisa Pochanard,<sup>3,4</sup> Eyal Mozes,<sup>1</sup> Levi A. Garraway,<sup>3,4</sup> and Dana Pe'er<sup>1,2,\*</sup>

<sup>1</sup>Department of Biological Sciences, Columbia University, 1212 Amsterdam Avenue, New York, NY 10027, USA

<sup>2</sup>Center for Computational Biology and Bioinformatics, Columbia University, 1130 St. Nicholas Avenue, New York, NY 10032, USA

<sup>3</sup>Department of Medical Oncology, Dana-Farber Cancer Institute, Harvard Medical School, 44 Binney Street, Boston, MA 02115, USA

<sup>4</sup>Broad Institute of Harvard and MIT, 7 Cambridge Center, Cambridge, MA 02142, USA

<sup>5</sup>These authors contributed equally to this work

\*Correspondence: [dpeer@biology.columbia.edu](mailto:dpeer@biology.columbia.edu)

DOI 10.1016/j.cell.2010.11.013

## SUMMARY

Systematic characterization of cancer genomes has revealed a staggering number of diverse aberrations that differ among individuals, such that the functional importance and physiological impact of most tumor genetic alterations remain poorly defined. We developed a computational framework that integrates chromosomal copy number and gene expression data for detecting aberrations that promote cancer progression. We demonstrate the utility of this framework using a melanoma data set. Our analysis correctly identified known drivers of melanoma and predicted multiple tumor dependencies. Two dependencies, *TBC1D16* and *RAB27A*, confirmed empirically, suggest that abnormal regulation of protein trafficking contributes to proliferation in melanoma. Together, these results demonstrate the ability of integrative Bayesian approaches to identify candidate drivers with biological, and possibly therapeutic, importance in cancer.

## INTRODUCTION

Large-scale initiatives to map chromosomal aberrations, mutations, and gene expression have revealed a highly complex assortment of genetic and transcriptional changes within individual tumors. For example, copy number aberrations (CNAs) occur frequently in cancer due to genomic instability. Genomic data have been collected for thousands of tumors at high resolution using array comparative genomic hybridization (aCGH) (Pinkel et al., 1998), high-density single-nucleotide polymorphism (SNP) microarrays (Beroukhi et al., 2010; Lin et al., 2008), and massively parallel sequencing (Plesance et al., 2010). Although multiple new genes have been implicated in cancer through sequencing and CNA analysis (Garraway et al., 2005), these studies have also revealed enormous diversity in genomic aberrations in tumors among individuals. Each tumor is unique and typically harbors a large number of genetic lesions,

of which only a few drive proliferation and metastasis. Thus, identifying driver mutations (genetic changes that promote cancer progression) and distinguishing them from passengers (those with no selective advantage) has emerged as a major challenge in the genomic characterization of cancer.

The most widely used approaches are based on the frequency that an aberration occurs: if a mutation provides a fitness advantage in a given tumor type, its persistence will be favored, and it is likely to be found in multiple tumors. For example, GISTIC identifies regions of the genome that are aberrant more often than would be expected by chance and has been used to analyze a number of cancers (Beroukhi et al., 2007, 2009; Lin et al., 2008). However, there are limitations to analytical approaches based on CNA data alone: CNA regions are typically large and contain many genes, most of which are passengers that are indistinguishable in copy number from the drivers. CNA data have statistical power to detect only the most frequently recurring drivers above the large number of unrelated chromosomal aberrations that are typical in cancer. Finally, these approaches rarely elucidate the functional importance or physiological impact of the genetic alteration on the tumor. These limitations highlight the need for new approaches that can integrate additional data to identify drivers of cancer. Gene expression is readily available for many tumors, but how best to combine it with information on CNA is not obvious.

We postulate that driver mutations coincide with a “genomic footprint” in the form of a gene expression signature. We developed an algorithm that integrates chromosomal copy number and gene expression data to find these signatures and identify likely driver genes located in regions that are amplified or deleted in tumors. Each potential driver gene is altered in some, but not all, tumors and, when altered, is considered likely to play a contributing role in tumorigenesis. Unique to our approach, each driver is associated with a gene module, which is assumed to be altered by the driver. We sometimes gain insight into the likely role of a candidate driver based on the annotation of the genes in the associated module. We demonstrate the utility of our method using a data set (Lin et al., 2008) that includes paired measurements of gene expression and copy number from 62 melanoma samples. Our analysis correctly identified known drivers of melanoma and connected them to many of their

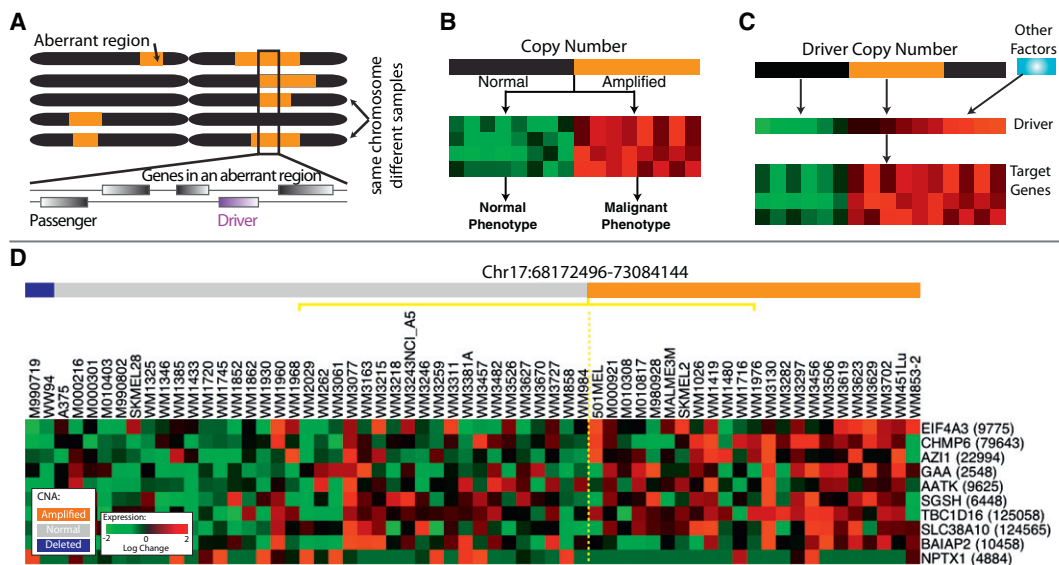


**Figure 1. Modeling Assumptions**

For all heat maps, each row represents a gene and each column represents a tumor sample.

(A) The same chromosome in different tumors; orange represents amplified regions. The box shows regions amplified in multiple tumors.

(B) An idealized signature in which the target genes are upregulated (red) when the DNA encoding the driver is amplified (orange).

(C) A driver may be overexpressed due to amplification of the DNA encoding it or due to the action of other factors. The target genes correlate with driver gene expression (middle row), rather than driver copy number (top row).

(D) Data representing amplified region on chromosome 17. Heat maps of expression for 10 of 24 genes that passed initial expression filtering (Extended Experimental Procedures).

Samples are ordered according to amplification status of the region (orange, amplified; blue, deleted). These genes are identical in their amplification status, and though gene expression is correlated with amplification status to some degree, the expression of each gene is unique. It is these differences that facilitate the identification of the driver. See also Extended Experimental Procedures, Figure S1, and Table S1.

targets and biological functions. In addition, it predicted novel melanoma tumor dependencies, two of which, *TBC1D16* and *RAB27A*, were confirmed experimentally. Both of these genes are involved in the regulation of vesicular trafficking, which highlights this process as important for proliferation in melanoma.

## RESULTS

### The Genomic Signature of a Driver

We define a “driver mutation” to be a genetic alteration that provides the tumor cell with a growth advantage during carcinogenesis or tumor progression (Stratton et al., 2009). We reasoned that driver mutations might leave a genomic “footprint” that can assist in distinguishing between driver and passenger mutations based on the following assumptions: (1) a driver mutation should occur in multiple tumors more often than would be expected by chance (Figure 1A); (2) a driver mutation may be associated (correlated) with the expression of a group of genes that form a “module” (Figure 1B); (3) copy number aberrations often influence the expression of genes in the module via changes in expression of the driver (Figure 1C).

Driver mutations are frequently associated with the abnormal regulation of processes such as proliferation, differentiation, motility, and invasion. Given that many cancer phenotypes are reflected in coordinated differences in the expression of multiple genes (a module) (Golub et al., 1999; Segal et al., 2004), a driver

mutation might be associated with a characteristic gene expression signature or other phenotypic output representing a group of genes whose expression is *modulated* by the driver. In addition, CNAs do not typically alter the coding sequence of the driver and so are expected to influence cellular phenotype via changes in the driver’s expression. In consequence, changes in expression of the driver are important, so approaches that measure association between the expression of a candidate driver (as opposed to its copy number) and that of the genes in the corresponding module are likely to promote the identification of drivers.

Gene expression is particularly useful for identifying candidate drivers within large amplified or deleted regions of a chromosome: whereas genes located in a region of genomic copy gain/loss are indistinguishable in copy number, expression permits the ranking of genes based on how well they correspond with the phenotype (Figure 1D). CNA data aids in determining the direction of influence, which cannot be derived based on correlation in gene expression alone (Figure 3A). This permits an unbiased approach for identifying candidate drivers from any functional family, beyond transcription factors or signaling proteins.

### A Bayesian Network-Based Algorithm to Identify Driver Genes

We developed a computational algorithm, copy number and expression in cancer (CONEXIC), that integrates matched copy

Gene Symbol	Pathway	Band	Genes in Region	Validation p-value
<b>MITF</b>	Melanoma	3p14.2-p14.1	1	<10 <sup>-6</sup>
TBC1D16	Vesicular Trafficking	17q25.3	24	<10 <sup>-6</sup>
ZFP106	Insulin/Ras	15q15.1	7	<10 <sup>-6</sup>
DIXDC1	Wnt/JNK/PI3K	11q23.1	17	0.0001
OIP5	Cell Cycle	15q15.1	13	<10 <sup>-6</sup>
TTBK2		15q15.2	7	0.0383
TRAF3	NFkappaB/JNK	14q32.32	19	0.0121
RAB27A	Vesicular Trafficking	15q15-q21.1	33	<10 <sup>-6</sup>
C12orf35		12p11.21	45	<10 <sup>-6</sup>
WBP2		17q25	92	0.0275
MOCS3		20q13.13	16	<10 <sup>-6</sup>
NDUFB2		7q34	10	<10 <sup>-6</sup>
ST6GALNAC2		17q25.1	92	<10 <sup>-6</sup>
GRB2	EGFR/Ras	17q24-q25	92	0.1373
ECM1		1q21	55	0.0083
KCNG1		20q13	16	0.202
DPM1		20q13.13	16	0.097
PFKP	Metabolism	10p15.3-p15.2	3	0.0801
<b>KLF6</b>	Cell cycle, c-JUN (JNK)	10p15	3	<10 <sup>-6</sup>
TIMM8B	Mitochondria	11q23.1-q23.2	17	0.7622
PI4KB		1q21	55	0.0003
PSMB4		1q21	55	0.0005
VPS72		1q21	55	<10 <sup>-6</sup>
TARS2		1q21.3	55	0.0001
MNS1		15q21.3	33	0.0908
TDRD3	RNA processing	13q21.2	203	<10 <sup>-6</sup>
CCNB2	Cell Cycle	15q22.2	33	<10 <sup>-6</sup>
EIF5	Cell Cycle	14q32.32	19	0.1096
RAB7A	Vesicular Trafficking	3q21.3	16	<10 <sup>-6</sup>
PIK3CB	PI3K signaling	3q22.3	15	<10 <sup>-6</sup>

number (amplifications and deletions) and gene expression data from tumor samples to identify driver mutations and the processes that they influence. CONEXIC is inspired by Module Networks (Segal et al., 2003) but has been augmented by a number of critical modifications that make it suitable for identifying drivers (see [Extended Experimental Procedures](#) available online). CONEXIC uses a score-guided search to identify the combination of modulators that best explains the behavior of a gene expression module across tumor samples and searches for those with the highest score within the amplified or deleted regions ([Extended Experimental Procedures](#) and [Figure S1](#)).

The resulting output is a ranked list of high-scoring modulators that both correlate with differences in gene expression modules across samples and are located in amplified or deleted regions in a significant number of these samples. The fact that the modulators are amplified or deleted indicates that they are likely to control the expression of the genes in the corresponding modules (see [Figure 3](#)). Because the modulators are amplified or deleted in a significant number of tumors, it is reasonable to assume that expression of the modulator (altered by copy number) contributes a fitness advantage to the tumor. Therefore, the modulators likely include genes whose alteration provides a fitness advantage to the tumor.

### Identifying Candidate Driver Genes in Melanoma

We applied the CONEXIC algorithm to paired gene expression and CNA data from 62 cultured (long- and short-term) mel-

### Figure 2. The Highest-Scoring Modulators Identified by CONEXIC

Gene names are color coded based on the role of the gene in cancer. Ten genes have been previously identified as oncogenes or tumor suppressors (blue); of these, two in melanoma (brown). Column 3 represents chromosomal location, orange represents amplification, and blue represents deletion. These genes were identified within regions containing multiple genes, and the number of genes in each aberrant region is listed in column 4. Column 5 lists the p value for modulator validation in independent data (for a full list, see [Table S2](#) and [Figure S3C](#)). p values are shown for the Johansson data set unless the modulator was missing from this data set, and then p value from the Hoek data set is shown. See also [Extended Experimental Procedures](#), [Table S2](#), and [Figure S3](#).

nomas (Lin et al., 2008). A list of candidate drivers was generated using copy number data available for 101 melanoma samples by applying a modified version (Sanchez-Garcia et al., 2010) of GISTIC (Beroukhi et al., 2007) (see [Table S1](#)). Next, we integrated copy number and gene expression data (available for 62 tumors) to identify the most likely drivers ([Extended Experimental Procedures](#)). Statistical power is gained by integrating all data and by combining statistical tests on thousands of genes to support the selected modulators. This resulted in the identification of 64 modulators that explain the behavior of 7869 genes. We consider the top 30 scoring modulators, presented in [Figure 2](#), as likely drivers (see [Table S2](#) for the complete list).

### Many Modulators Are Involved in Pathways Related to Melanoma

The top 30 modulators (likely drivers) include 10 known oncogenes and tumor suppressors ([Figure 2](#)). In many cases, CONEXIC chose the cancer-related gene out of a large aberrant region containing many genes. For example, *DIXDC1*, a gene known to be involved in the induction of colon cancer (Wang et al., 2009b), was selected among 17 genes in an aberrant region ([Figure S2](#)). *CCNB2*, a cell-cycle regulator, was selected from a large amplified region containing 33 genes. The modulators span diverse functional classes, including signal transducers (*TRAF3*), transcription factors (*KLF6*), translation factors (*EIF5*), and genes involved in vesicular trafficking (*RAB27A*).

Performing a comprehensive literature search for all genes is tedious and time consuming, so we developed an automated procedure, literature vector analysis (LitVAn), which searches for overrepresented terms in papers associated with genes in a gene set. LitVAn uses a manually curated database (NCBI Gene) to connect genes with terms from the complete text of more than 70,000 published scientific articles ([Extended Experimental Procedures](#)). LitVAn found a number of overrepresented terms ([Figure S3E](#)) among the top 30 modulators, including “PI3K” and “MAPK,” which are known to be activated in melanoma; “cyclin,” representing proliferation, which is common in

all cancers; and “RAB.” Rabs regulate vesicular trafficking, a process not previously implicated in melanoma.

### The Association between a Modulator and the Genes in a Module

Beyond generating a list of likely drivers (modulators), the CONEXIC output includes groups of genes that are associated with each modulator (modules). We tested how reproducible the modulators and their associated modules are using gene expression data from two other melanoma cohorts with 45 (Hoek et al., 2006) and 63 (Johansson et al., 2007) samples (see [Extended Experimental Procedures](#) and [Figure S3](#)). We found that 51 of 64 (80%) of the selected modulators are conserved across data sets in a statistically significant manner. Modules (statistically associated genes) are likely enriched with genes whose expression is biologically affected by the modulator ([Figure 3](#)). In consequence, the processes and pathways represented by genes in a module can help us to gain insight into how an aberration in the modulator might alter the cellular physiology and contribute to the malignant phenotype.

Annotation of data-derived sets of genes is typically carried out based on gene set enrichment using Gene Ontology (GO) annotation. Although this approach is useful, there are modules for which GO annotation does not capture the known biology. For example, the “TNF module” is enriched with the GO terms “developmental process” and “cell differentiation” (q value = 0.0014 and 0.004, respectively). We used LitVAN to carry out a systematic literature search and found 11 of 20 genes in the module related to the TNF pathway, inflammation, or both ([Figure 3C](#) and [Table S3](#)), although only two of these genes were annotated for these processes in GO. *TRAF3*, the modulator chosen by CONEXIC, is known to regulate the NF- $\kappa$ B pathway (Vallabhapurapu et al., 2008), a major downstream target of TNF. Although *TRAF3* has not been previously implicated in melanoma, the importance of the NF- $\kappa$ B pathway in melanoma is well supported (Chin et al., 2006).

### A Known Driver, MITF, Is Correctly Associated with Target Genes

CONEXIC identified microphthalmia-associated transcription factor (*MITF*) as the highest-scoring modulator. *MITF* is a master regulator of melanocyte development, function, and survival (Levy et al., 2006; Steingrímsson et al., 2004), and the overexpression of *MITF* is known to have an adverse effect on patient survival (Garraway et al., 2005).

To test the association between modulator and module, we obtained an experimentally derived list of *MITF* targets (Hoek et al., 2008b) and asked whether the modules identified by CONEXIC associate *MITF* with its known targets. The *MITF*-associated modules contained 45 of 80 previously identified targets (p value <  $1.5 \times 10^{-45}$ ) supporting a match between the transcription factor (TF) and its known targets. However, a few targets (*TBC1D16*, *ZFP106*, and *RAB27A*) are both associated with *MITF* and are themselves modulators of additional modules. CONEXIC limits each gene to a single module, so association with an *MITF* target would preclude association with *MITF*. If we permit indirect association to *MITF* through the modules of these additional modulators, CONEXIC correctly identifies 76 of

the 80 targets identified by Hoek et al. (p value <  $1.5 \times 10^{-78}$ ). Similar target sets are not available for any other modulator, precluding a more rigorous evaluation of our other predictions.

### MITF Expression Correlates with Targets Better Than Copy Number

Expression of *MITF* correlates with the expression of its targets better than *MITF* copy number, though both correlations are statistically significant (p value of 0.0001 versus 0.04; [Figures 4A](#) and [4B](#)). This relationship is unidirectional: *MITF* is significantly overexpressed when its DNA is amplified (p value 0.0004), but overexpressed *MITF* does not always correspond with *MITF* amplification. We find that *MITF* is less correlated with its copy number (rank 294th) than most other genes in aberrant regions (see [Table S1C](#)), and more than half of the tumors that overexpress *MITF* do not have a CNA that spans the *MITF* gene. Comparison of *MITF* target expression between samples with and without *MITF* amplification did not show an effect of DNA amplification on expression of the targets ([Extended Experimental Procedures](#)).

### MITF Correctly Annotated with Its Known Role in Melanoma

We used GO gene set enrichment to identify the biological processes and pathways represented in each module associated with *MITF*. The module containing the genes most significantly upregulated by *MITF* ([Figure 4B](#) and [Figure S4A](#)) is significantly enriched for the terms “melanosome” and “pigment granule” (q value =  $4.86e^{-6}$  for each). It includes targets involved in proliferation such as *CDK2*, consistent with the observation that *MITF* can promote proliferation via lineage-specific regulation of *CDK2* (Du et al., 2004). The module containing genes most strongly inhibited by *MITF* ([Figure 4B](#) and [Figure S4B](#)) has a metastatic signature strongly associated with invasion, angiogenesis, the extracellular matrix, and NF- $\kappa$ B signaling. These modules and their annotation suggest that *MITF* serves as a developmental switch between two types of melanoma, in which high *MITF* expression promotes proliferation and low *MITF* expression promotes invasion. Thus, our automated, computationally derived findings dissect a complex response and accurately recapitulate the known literature, including the experimental characterization of *MITF* (Hoek et al., 2008a).

LitVAN annotated additional modulators with their known role (e.g., *CCNB2* with cell cycle and mitosis; data not shown). The detailed match between the CONEXIC output and empirically derived knowledge of the role of known modulators in melanoma provides confidence in CONEXIC’s predictions for modulators that are not well characterized.

### Identification of *TBC1D16* as a Tumor Dependency in Melanoma

The second highest-scoring modulator identified by CONEXIC is *TBC1D16*, a Rab GTPase-activating protein of unknown biological function. Rabs are small monomeric GTPases involved in membrane transport and trafficking. *TBC1D16* is well conserved, and although its targets are not known, a close paralog, *TBC1D15*, regulates *RAB7A* (also selected as a modulator; [Figure 2](#)) (Itoh et al., 2006). We used a module associated with *TBC1D16* to infer its potential role in melanoma ([Figure 5A](#))

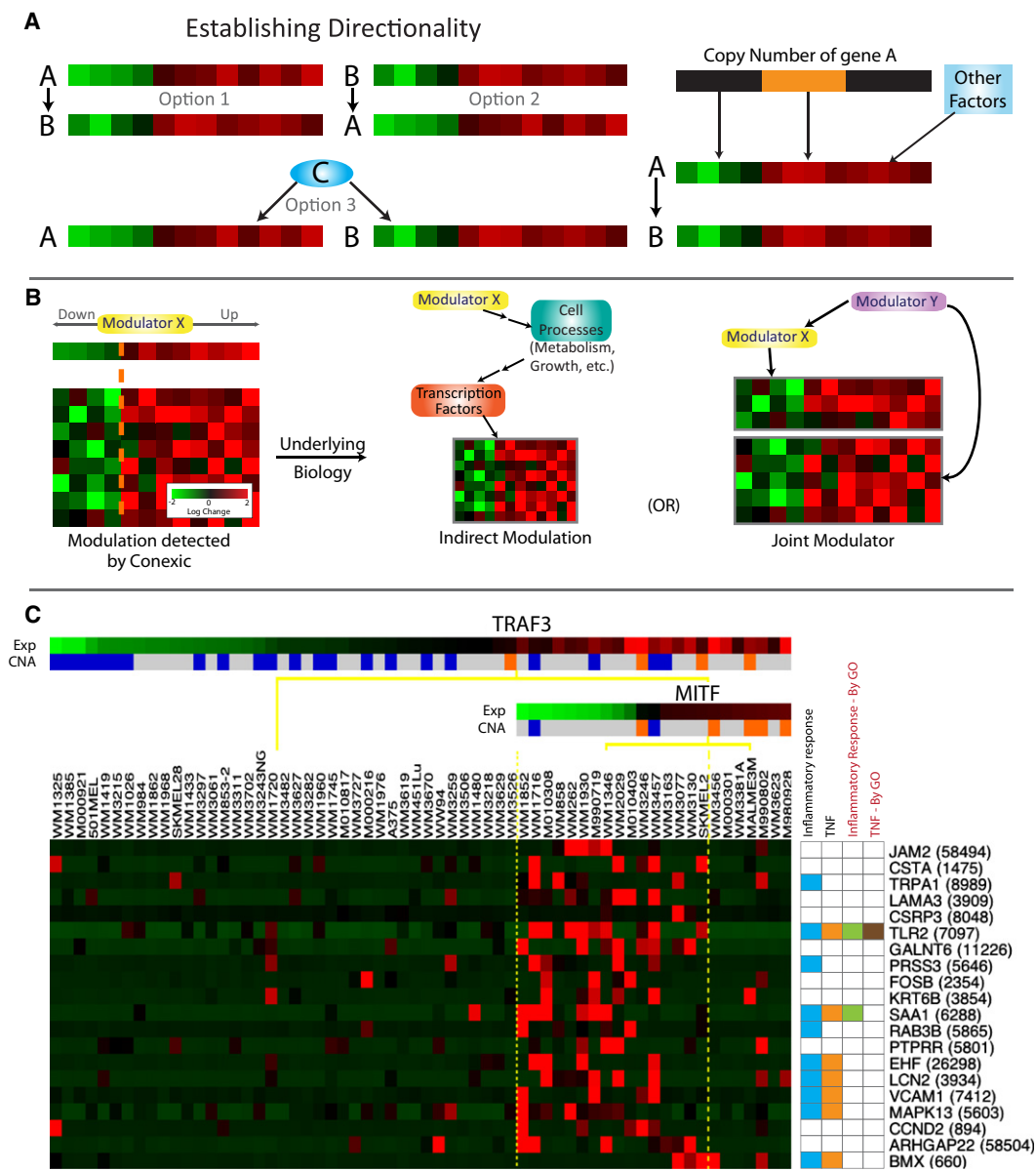


**Figure 3. Associating Modulators to Genes**

(A) Three scenarios could explain a correlation between a candidate driver (gene A) and its target (gene B): A could influence B, B could influence A, or both could be regulated by a common third mechanism (Pearl, 2000). The availability of both gene expression and chromosomal copy number data allows us to establish the likely direction of influence. If the expression of gene A is correlated with its DNA copy number and the copy number is altered in a large number of tumors, it is likely that the copy number alteration results in a change in expression of A in these tumors. So the model in which A influences the expression of B and other correlated genes is the most likely. In this way, examination of both copy number and gene expression in a single integrated computational framework facilitates identification of candidate drivers.

(B) Modulator influence on a module can go beyond direct transcriptional cascades involving transcription factors or signaling proteins and their targets. Genetic alteration of any gene (e.g., a metabolic enzyme) can alter cell physiology, which is sensed by the cell and subsequently leads to a transcriptional response through a cascade of indirect influences and mechanisms. Whereas modules are typically enriched for genes influenced by the modulator, they also contain genes that are coexpressed with the modulator (“joint modulator”). Both types are helpful for annotating the module and determining the functional role of the modulator.

(C) The TNF module. The modulators include *TRAF3* and *MITF*, wherein high *TRAF3* and low *MITF* are required for upregulation of the genes in the module. The annotation for each gene is represented in a color-coded matrix. Blue and orange squares represent literature-based annotation (see Table S3); green and brown are from GO. LitVAN associated the genes in this module with TNF and the inflammatory response.

See also Figure S2 and Table S3.

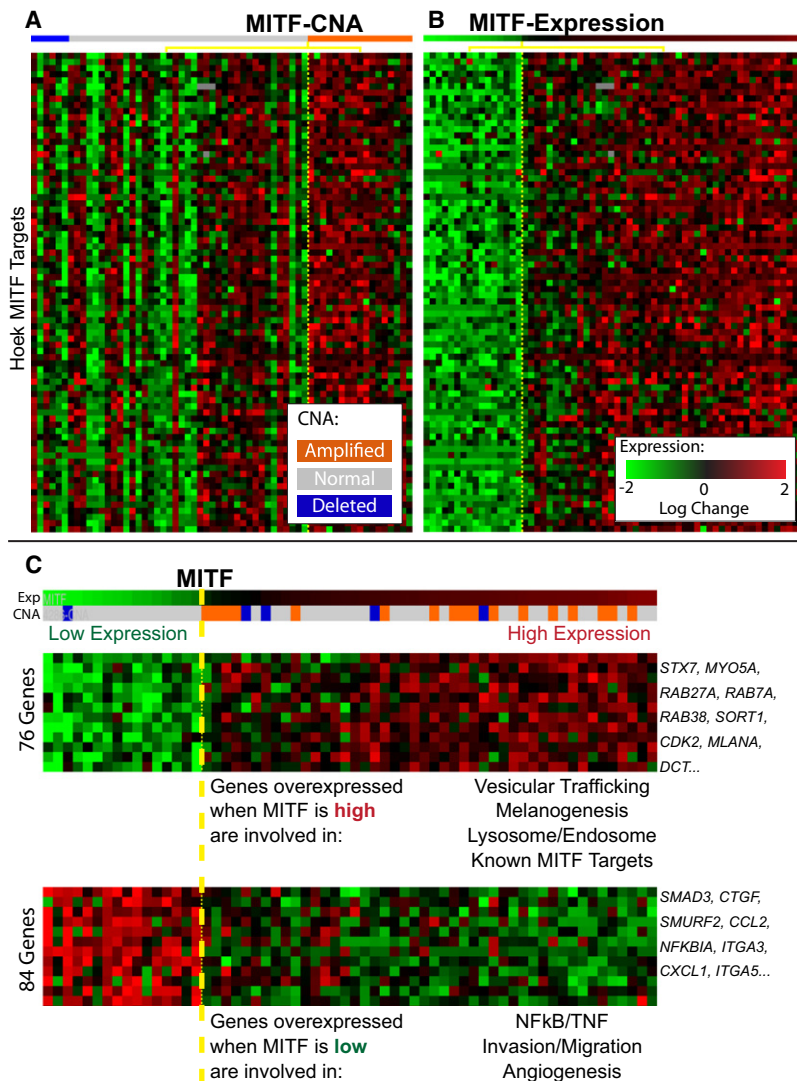


**Figure 4. MITF Expression Correlates with Expression of the Genes in the Associated Module**

(A) Each row represents the gene expression of 1 of 78 MITF targets identified by Hoek (Hoek et al., 2008b); the tumor samples are split into two groups based on the copy number of *MITF* (Welch t test p value = 0.04).

(B) The rows represent the same genes, in the same order as in (A), but here, the tumor samples are split into a group of samples that express *MITF* at high ( $n = 46$ ) or low levels ( $n = 16$ ) (Welch t test p value = 0.0001).

(C) Two modules associated with *MITF*, showing a selected subset of genes. LitVAN annotation for the genes in each module is shown below the heat map. The complete modules with all genes are available in Figure S4.

We carried out western blotting and RT-PCR on some of the short-term cultures (STCs) used to generate the Lin data set and asked whether the *TBC1D16* transcript correlates with protein levels. The results confirmed that the expression of *TBC1D16* corresponds well with the amount of the 45 kD isoform of *TBC1D16* (data not shown). These results suggest that knockdown of *TBC1D16* expression in tumors that have high levels of *TBC1D16* will lead to a reduction in proliferation.

#### ***TBC1D16* Is Required for Proliferation**

To test whether *TBC1D16* is required for proliferation of melanoma cultures, we carried out a knockdown experiment. We selected two STCs with high levels of *TBC1D16*, WM1960 (16-fold higher expression than WM1346, DNA not amplified) and WM1976 (34-fold higher expression, amplified DNA) and control STCs, WM262 and WM1346 that express *TBC1D16* at a lower level. We used two shRNAs to knock down *TBC1D16* expression in each of the four STCs and measured growth over 8 days (Extended Experimental Procedures). RT-PCR

and discovered that diverse biological processes are represented by genes in the module and that more than half are annotated for processes such as melanogenesis, vesicular trafficking, and survival/proliferation (Table S4A). This suggests that *TBC1D16* plays a role in cell survival and proliferation.

*TBC1D16* is an uncharacterized gene located in an amplified region that contains 23 other genes, including *CBX4*, which is known to play a role in cancer (Satijn et al., 1997). Expression of *TBC1D16* is not highly correlated with *TBC1D16* copy number compared to other genes in the region (ranked 7th out of 24) or to all candidate drivers (252th out of 428). Nevertheless, *TBC1D16* is the top-scoring gene in the region and the second highest-scoring modulator, so it was selected for experimental verification.

The module exhibits a dose-response relationship between *TBC1D16* expression and the expression of genes in the module such that higher expression of *TBC1D16* is correlated with higher expression of genes in the module (correlation coefficient 0.76).

was used to confirm that the reduction in the amount of the *TBC1D16* transcript was similar for all of the STCs (Figure S5). Knockdown of *TBC1D16* expression reduced cell growth in WM1960 and WM1976 to 16% and 40%, respectively, relative to controls infected with GFP shRNA in the same STCs (Figures 5B–5D). This result is specific for cultures with high levels of *TBC1D16*, as the controls, WM262 and WM1346, grow at similar rates to cultures infected with shGFP (75%–90%). As predicted, growth inhibition at day 8 is proportional to the amount of the *TBC1D16* transcript and is independent of *TBC1D16* copy number (Figures 5C and 5D). Taken together, these results support CONEXIC's prediction that *TBC1D16* is required for proliferation in melanomas that overexpress the gene.

#### ***RAB27A* Identified and Experimentally Confirmed as a Tumor Dependency**

The *TBC1D16* module contains a second modulator, *RAB27A*, also known to be involved in vesicular trafficking (Figure 5A).

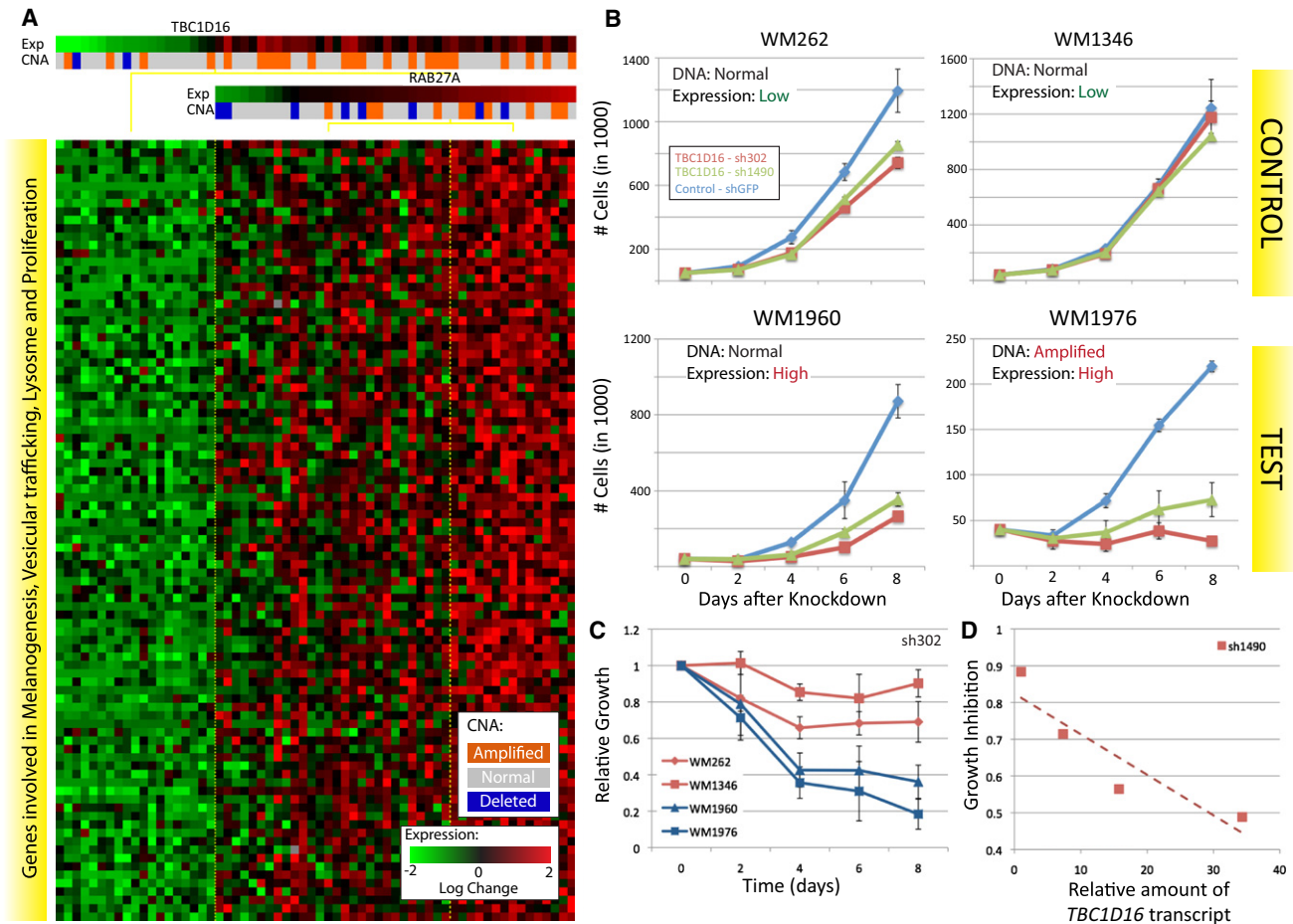


**Figure 5. *TBC1D16* Is Necessary for Melanoma Growth**

(A) A module associated with *TBC1D16* and *RAB27A*. The genes in the module are involved in melanogenesis, survival/proliferation, lysosome, and protein trafficking (see Table S4A for details).

(B) Representative growth curves for each of the four STCs infected with *TBC1D16* shRNA. Each curve represents three technical replicates. RT-PCR was used to confirm that the reduction in the amount of the *TBC1D16* transcript was similar for all of the STCs (Figure S5).

(C) Change in growth over time, relative to the number of cells plated, averaged over all replicates (Extended Experimental Procedures). Mean over three biological replicates  $\times$  three technical replicates for each STC. See Figure S5 and Table S4B for additional replicates and hairpins.

(D) Growth inhibition at 8 days is directly proportional to the amount of the *TBC1D16* transcript and is independent of the *TBC1D16* copy number.

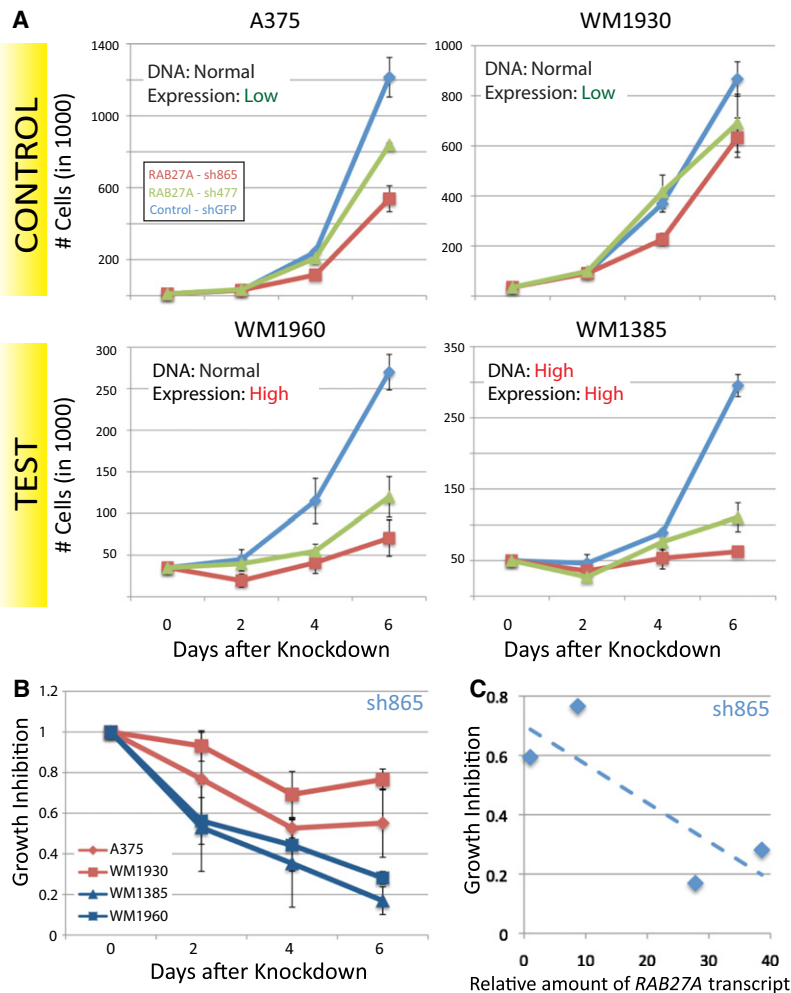
*RAB27A* functions with *RAB7A* to control melanosome transport and secretion. *RAB7A* localizes to early melanosomes, whereas *RAB27A* is found in mature melanosomes (Jordens et al., 2006). CONEXIC selected both *RAB27A* and *RAB7A* as modulators.

*RAB27A* is in an amplified region that did not pass the standard GISTIC q value threshold for significance, and expression of the gene is not highly correlated with *RAB27A* copy number compared to other candidate drivers (323th out of 428). Nevertheless, CONEXIC identified it as the top-scoring modulator out of the 33 genes in this region and ranked it 8th out of 64 modulators, and it was therefore selected for empirical assessment.

To test the prediction that *RAB27A* is important for proliferation in tumors with high levels of *RAB27A*, we tested the effect of shRNA knockdown of the *RAB27A* transcript on proliferation. We chose two STCs in which the gene is highly expressed WM1385 (28-fold higher expression compared with A375, DNA

amplified) and WM1960 (38-fold higher expression, DNA not amplified) and two controls that express *RAB27A* at a lower level (A375 and WM1930). Western blots show that expression of *RAB27A* correlates with expression of the cognate gene in these cultures (data not shown).

Knockdown of *RAB27A* expression using shRNA was similar for all cultures (Figure S6) but only reduced cell growth significantly in the STCs that overexpress *RAB27A* (18% or 35% in WM1385 or WM1960 relative to the same cultures infected with GFP shRNA). *RAB27A* shRNA had less impact (growth rates of 65%–80%) in the control STCs that have low *RAB27A* (Figures 6A and 6B). Growth inhibition at 6 days is correlated with the amount of the *RAB27A* transcript and is independent of *RAB27A* copy number (Figures 6B and 6C). Taken together, these results support CONEXIC's prediction that *RAB27A* is a tumor dependency in melanomas that overexpress *RAB27A*.



### **RAB27A Affects the Expression of Genes in Associated Modules**

To test whether *RAB27A* affects the expression of genes in associated modules, as predicted by CONEXIC, we carried out microarray profiling after knockdown of *RAB27A* in the test STCs (WM1385 and WM1960). We compared the expression profile after *RAB27A* knockdown to a control profile generated by infecting the same STC with GFP shRNA. We used gene set enrichment analysis (GSEA) (Subramanian et al., 2005) to test whether each of the three modules associated with *RAB27A* are enriched with genes that are differentially expressed (DEG) after knockdown (see Extended Experimental Procedures). We found that all three *RAB27A*-associated modules are significantly enriched for genes affected by *RAB27A* ( $p$  values  $< 10^{-5}$  for all three modules; see Figure 7C) and that these modules responded in the direction predicted by CONEXIC.

These results support our computational prediction that the expression of *RAB27A* affects the expression of the genes in the associated modules. We note that *RAB27A* functions as a vesicular trafficking protein, suggesting that it influences gene expression through an unknown and likely indirect mechanism.

### **Figure 6. RAB27A Is Necessary for Melanoma Growth**

(A) Representative growth curves for each of the four STCs infected with *RAB27A* shRNA. Each curve represents three technical replicates. RT-PCR was used to confirm that the reduction in the amount of the *RAB27A* transcript was similar in all of the STCs (Figure S6).

(B) Change in growth over time, relative to the number of cells plated, averaged over all replicates. Knockdown of *RAB27A* expression in cells that express this gene at high levels reduces proliferation. Data averaged over three biological replicates  $\times$  three technical replicates for each STC. See Figure S6 and Table S5 for all data.

(C) Growth inhibition at 6 days is dependent on the amount of the *RAB27A* transcript and is independent of *RAB27A* copy number.

We used LitVAN to identify the biological processes and pathways represented among the DEGs. Cell cycle-related terms are significant among the downregulated genes, which might be expected given the reduced growth after *RAB27A* knockdown. In addition, we found that genes annotated for the ERK pathway are upregulated (including *MYC*, *FOSL1*, and *DUSP6*). We used GSEA to measure enrichment of an experimentally derived set of genes that respond to MEK inhibition in melanoma (Pratilas et al., 2009). The resulting  $p$  value  $< 4.7 \times 10^{-5}$  suggests that ERK signaling is altered after *RAB27A* knockdown in these STCs.

### **TBC1D16 Influences the Expression of Genes in Associated Modules**

We carried out microarray profiling after knockdown of *TBC1D16* to evaluate whether expression of *TBC1D16* affects the expression of genes in the four modules associated with it. We used two shRNAs to knock down *TBC1D16* in the test STCs (WM1960 and WM1976) and compared the gene expression to controls infected with GFP shRNA (in the same STCs). GSEA analysis established that all four modules are significantly enriched for genes affected by differences in *TBC1D16* expression ( $p$  values  $< 10^{-5}$ , 0.0002, 0.008, and 0.009, respectively; see Figure 7). Two modules responded to *TBC1D16* knockdown in the direction predicted by CONEXIC. In addition, GSEA analysis ranked genes in the *TBC1D16* module (Module 25) highest out of 177 (based on the GSEA  $p$  value), demonstrating that the genes in this module are the most highly differentially expressed genes in the data set.

The function of *TBC1D16* is unknown, but it is predicted to be involved in vesicular trafficking. In our knockdown analysis, LitVAN annotated the upregulated genes with terms related to vesicular trafficking. These include *RAB3C*, *RAB7A*, *CHMP1B*, *RAB18*, *SNX16*, *COPB1*, and *CAV1* (see Table S6A). However, it is not clear how *TBC1D16* affects gene expression or how changes in expression affect vesicular trafficking.

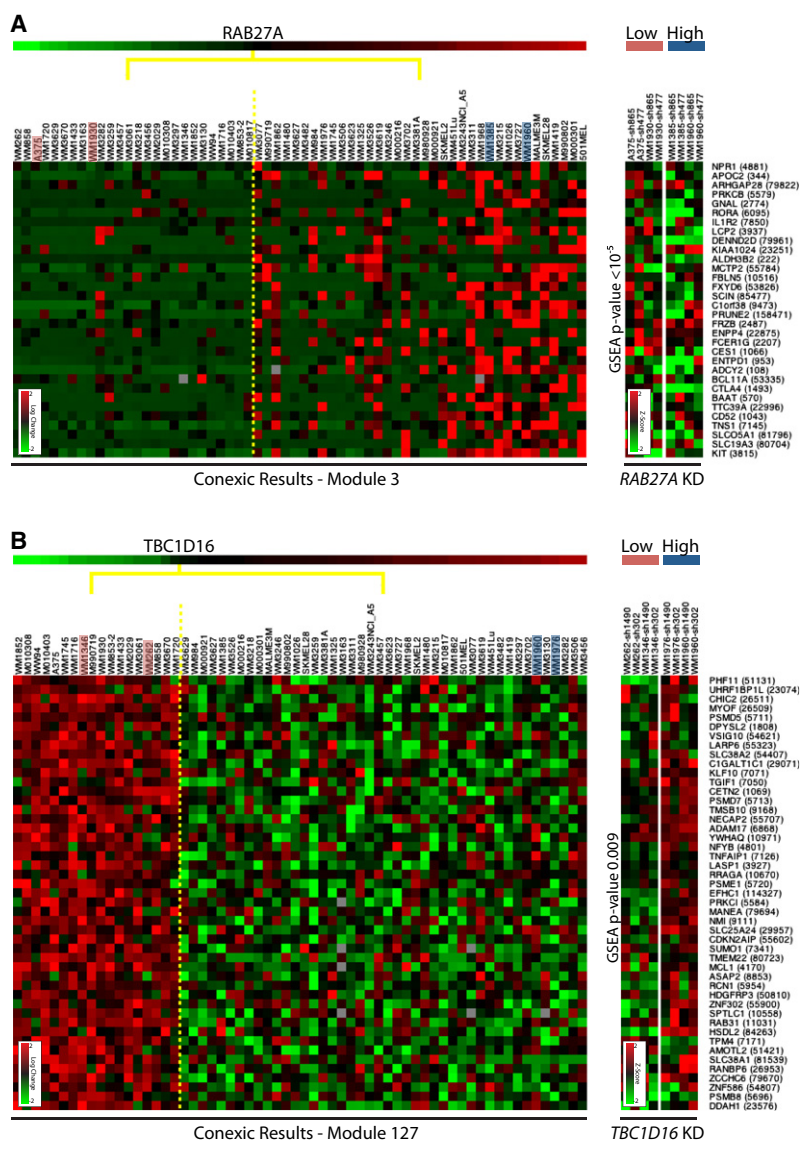


**Figure 7. Results of Knockdown Microarrays for RAB27A and TBC1D16**

(A) To the left is one of the modules associated with RAB27A, and to the right are data generated following knockdown (KD) of RAB27A for the same genes in the STCs indicated (pink and blue). The expression of genes in the module goes down relative to shGFP, as predicted. KD expression heat map shows Z scores (see Extended Experimental Procedures) showing that these are some of the most differentially expressed genes (DEGs) in the genome.

(B) To the left is one of the modules associated with TBC1D16, and to the right are data generated following KD of TBC1D16 in the STCs indicated. The expression of genes in the module goes up relative to shGFP, as predicted. The test STCs (blue) and control STCs (pink) respond differently, demonstrating the importance of context (TBC1D16 overexpression status) in determining the response.

(C) GSEA p value and ranking (relative to 177 CONEXIC modules) for RAB27A- and TBC1D16-associated modules (see Figure S7 for data). GSEA was calculated using the median of four profiles (two cell lines x two hairpins) on the test STCs. Significant p values indicate that knockdown of RAB27A and TBC1D16 each affects the subset of genes predicted by CONEXIC (note that  $10^{-5}$  is the smallest p value possible given that 100,000 permutations are used). The color of the module name represents the predicted direction of response to knockdown (red and green represent up- and downregulated, respectively). The arrow represents the observed response to knockdown. The direction of response was correctly predicted for two of four TBC1D16 modules and for all RAB27A modules.

See also Figure S7 and Table S6.

and to identify those that are likely to be drivers. The combination of data types allows us to identify regions that would be overlooked using methods based on DNA copy number alone.

**Expression of a Driver, Not Its Copy Number, Drives Phenotype**

The novelty of our method and the key to its success is our modeling paradigm: the expression of a driver should correspond with the expression of genes in an associated module. Examination of MITF and its targets supports our assumptions. Expression of MITF best correlates with the expression of its targets, but MITF overexpression does not always correspond with MITF amplification. A change

in DNA copy number is only one of many ways that gene expression can be altered. For example, MITF expression can be upregulated via signaling from the Ras/Raf (oncogenic BRAF occurs frequently in melanoma) (Wellbrock et al., 2008) and Frizzled/Wnt pathways (Chin et al., 2006).

Most methods for identifying drivers within aberrant regions focus on genes whose expression is well correlated with the copy number of the cognate DNA (Lin et al., 2008; Turner

**C**

RAB27A Moduled Modules

Module	GSEA p-value	Rank
Module 3	<math><10^{-5}</math>	3 ↓
Module 31	<math><10^{-5}</math>	2 ↑
Module 75	<math><10^{-5}</math>	7 ↓

TBC1D16 Moduled Modules

Module	GSEA p-value	Rank
Module 25	<math><10^{-5}</math>	1 ↓
Module 75	0.008	21 ↓
Module 147	<math>2 \times 10^{-5}</math>	5 ↓
Module 127	0.009	22 ↑

**DISCUSSION**

We have demonstrated that combining tumor gene expression and copy number data into a single framework increases our ability to identify likely drivers in cancer and the processes affected by them. Gene expression allows us to distinguish between multiple genes in an amplified or deleted region (many of which are indistinguishable based on copy number)

et al., 2010). The expression of many of the predicted drivers that we identify is poorly correlated with their copy number, relative to other genes in the region and to all other candidate drivers *MITF* (294th), *TBC1D16* (252th) and *RAB27A* (323th) (see Table S1C). We believe that the discrepancies between CNA and expression arise because there are multiple ways to up- or downregulate a gene. For example, *TBC1D16* and *RAB27A* were both identified as transcriptional targets of MITF (Chiaverini et al., 2008; Hoek et al., 2008b) and are therefore upregulated when *MITF* is overexpressed. Moreover, we postulate that many drivers are less correlated with their copy number than passengers due to selective pressure; if there is a fitness advantage to up- or downregulate expression, the tumor will find a mechanism to do so.

### ***TBC1D16* and *RAB27A* Are Required for Proliferation**

We tested two drivers predicted by CONEXIC with knockdown experiments and showed that tumors that express either *TBC1D16* or *RAB27A* at high levels are dependent on the corresponding gene for growth. Our results demonstrate that these dependencies are determined by expression of the gene (in both cases), rather than DNA amplification status, further supporting the assumptions underlying our approach. Thus, we not only identify tumor dependencies, but also the tumors in which these genes are crucial for proliferation. Identifying dependencies that are critical for tumor survival is needed for drug-targeted therapies; for example, FLT3 inhibitors in AML, which have had successful phase II trials (Fischer et al., 2010). Our approach is unbiased with respect to protein function and does not incorporate prior knowledge, thus enabling the identification of dependencies in genes involved with vesicular trafficking. *TBC1D16* and *RAB27A* validate the ability of our approach to correctly identify tumor dependencies and the genes that they affect.

### **Association between Modulator and Module**

A key feature of our approach is that CONEXIC goes beyond identifying drivers. By associating candidate drivers with gene modules and annotating them using information from the literature, CONEXIC provides insight into the physiological roles of drivers and associated genes. We used LitVAn to find biological processes and pathways overrepresented in each module and to associate drivers with functions, accurately identifying targets of *MITF* and annotating the functions of known drivers (*MITF*, *CcBN2*, and *TRAF3*).

The results of microarray profiling following knockdown further support the association between modulator and module and confirm our ability to identify genes affected by *TBC1D16* and *RAB27A*. We successfully connected genes involved in vesicular trafficking to their effects on gene expression, likely through a cascade of indirect influences. In addition to profiling the STCs that highly express each of these genes (test STCs), we also profiled two lower-expressing STCs (control STCs), in which the effect of knockdown is less detrimental to growth. For *TBC1D16*, there is substantial overlap in the DEGs in the test STCs ( $p$  value  $< 6.6 \times 10^{-22}$ ), but not in the DEGs between control and test STCs ( $p$  value  $> 0.76$ ). This reflects the complexity of the transformed state and demonstrates that

genetic context has a fundamental impact on the effect of a perturbation.

### **Genes Involved in Trafficking Are Important in Melanoma**

Of the top 30 drivers selected by CONEXIC, three genes (*TBC1D16*, *RAB27A*, and *RAB7A*) are known to be involved in vesicular trafficking (Itoh et al., 2006; Jordens et al., 2006). All of these genes are amplified (DNA) and highly expressed (RNA) in multiple melanomas. There is increasing evidence that genes controlling trafficking play a role in melanoma. Germline variation in *Golgi phosphoprotein 3 (GOLPH3)*, a gene involved in vesicular trafficking, is associated with multiple cancers (Scott et al., 2009). Our data identify two novel dependencies that are encoded in somatic CNAs, demonstrate the dependency of melanoma on *TBC1D16* and *RAB27A* expression for proliferation, and highlight the potential role of vesicular trafficking in this malignancy.

The role of vesicular trafficking in melanoma has yet to be characterized. Vesicular trafficking regulates many receptor tyrosine kinases (RTKs) both spatially and temporally and thus determines both the duration and intensity of signaling (Ying et al., 2010). For example, *RAB7A* is involved in the regulation of ERK signaling (Taub et al., 2007), and ERK is known to play an important role in melanoma (Chin et al., 2006). Tight control of ERK expression could potentially be important in melanocytes because of its influence on MITF: ERK is required for the activation of MITF, but high levels of ERK lead to MITF degradation (Wellbrock et al., 2008). It is possible that recurrent aberrations in vesicular trafficking genes might involve control of ERK signaling intensity. This is further supported by the upregulation of an ERK signature (Pratilis et al., 2009) following *RAB27A* knockdown in our data ( $p$  value  $< 4.7 \times 10^{-5}$ ).

### **CONEXIC and Other Approaches**

CONEXIC differs from other methods in a number of ways. First, it uses the gene expression of a candidate driver, rather than its copy number, as a proxy to report on the status of the gene, e.g., two tumors that overexpress a driver are treated equivalently even if there is amplification in the DNA of only one of them. Second, it associates a candidate driver with a module of genes whose expression corresponds with that of the predicted driver, which was critical for identification of *TBC1D16* as a modulator. Third, combining copy number and gene expression provides greater sensitivity for identifying significantly aberrant regions that would not be selected based on DNA alone; this was critical for the identification of *RAB27A*.

Methods based on copy number data are limited to detecting large regions containing multiple genes, such that the driver cannot be readily identified among them. Recent efforts have focused on integrating additional sources of information into the analysis. Some methods use prior information, such as the role of a gene in other cancers (Beroukhim et al., 2010). Others, like CONEXIC, integrate gene expression data (Adler et al., 2006), but the results of these methods fall short of CONEXIC's. We systematically compared CONEXIC to other methods using the same data and found that they did not identify *MITF* or any other known driver in melanoma (see Extended Experimental Procedures).

Statistical dependencies in gene expression have been used to connect a regulator to its target (Friedman et al., 2000; Lee et al., 2006; Segal et al., 2003) and for uncovering important regulators in cancer (Adler et al., 2006; Carro et al., 2010; Wang et al., 2009a). These approaches typically only detect transcription factors and signaling molecules and do not connect the altered regulatory networks to upstream genetic aberrations. Incorporating information on amplification or deletion status allows us to consider any functional class of genes and thus permits detection of vesicular trafficking genes that would not be identified using other methods. It also allows us to relate the malignant phenotype to genetic aberrations from which it is likely to have originated.

We tuned our method toward reducing the selection of modulators that are not drivers. To gain this specificity, we do not detect all genes and pathways that drive tumors. First, some drivers in amplified and deleted regions do not pass the stringent statistical tests employed in our method. Second, CONEXIC only identifies candidate drivers that are encoded in amplified or deleted regions. In consequence, it would not detect drivers of melanoma such as *BRAF* and *NRAS* that are typically associated with point mutations. Third, CONEXIC detects drivers based on the assumptions delineated above; though these hold for many drivers, it is likely that they are not appropriate for all drivers.

To meet the challenge of finding all driving alterations in cancer, a number of complementary approaches are needed. Experimental approaches such as screening using pooled short hairpin RNAs (shRNAs) (Bric et al., 2009; Zender et al., 2008) are likely to detect a set of drivers different from those detected by CONEXIC. These screens are dependent on the genetic background and are limited to drivers that influence processes that can be readily measured, such as proliferation, whereas CONEXIC scans all of the genetic data together and can potentially identify drivers of any function across different genetic backgrounds. In the future, we envision that CONEXIC will be used to guide in vivo screening initiatives and to assist in the choice of regions, functional assays, and genetic backgrounds probed.

### Beyond Melanoma

The challenge of finding candidate drivers is considerable: tumors are heterogeneous, the data are noisy and highly correlated, and there are a large number of possible combinations of drivers and genes in modules. Our approach is successful because it couples simple modeling assumptions with powerful computational search techniques and rigorous statistical evaluation of the results at each step.

Both the principles underlying CONEXIC and the software can be applied to any tumor cohort containing matched data for copy number aberrations and gene expression. The principle of associating any type of mutation (e.g., epigenetic alterations and coding sequence) with gene expression signatures or other phenotypic outputs that differ among samples will be of increasing importance as sequence and epigenetic data accumulate. Not only does this help to distinguish between driver and passenger mutations, but the genes in the associated module can also provide insight into the role of the driver. This approach can be used to identify the genetic aberrations respon-

sible for tumorigenesis and to find those that relate to any other measurable phenotype, such as the resistance of tumors to drugs. We anticipate that our approach will make an important contribution toward a basic mechanistic understanding of cancer and in revealing associations of clinical significance. Cancer is a heterogeneous disease in which we are only just beginning to appreciate the importance of genetic background and the myriad ways in which the cellular machinery can be re-directed toward the transformed state. Methods that begin to dissect this complexity move us another step closer to a world where personalized therapies are routine.

## EXPERIMENTAL PROCEDURES

### Statistical Methods

A detailed description of the statistical methods and computational algorithms used can be found in the [Extended Experimental Procedures](#). The CONEXIC and LitVAN algorithms were developed for this research, and the software is available at <http://www.c2b2.columbia.edu/danapeerlab/html/software.html>.

### Experimental Methods

Cells were grown using standard culture conditions, and knockdown was carried out by infection with lentivirus using RNAi sequences designed by the RNAi Consortium. shRNA lentivirus were prepared according to TRC protocols (<http://www.broadinstitute.org/rnai/trc>), with minor modifications. Cell proliferation assays, RT-PCR, microarrays, and immunoblotting were carried out using standard techniques. Primer sequences and detailed methods can be found in the [Extended Experimental Procedures](#).

## ACCESSION NUMBERS

All primary data are available at the Gene Expression Omnibus (GSE23884).

## SUPPLEMENTAL INFORMATION

Supplemental Information includes [Extended Experimental Procedures](#), eight figures, and six tables and can be found with this article online at [doi:10.1016/j.cell.2010.11.013](https://doi.org/10.1016/j.cell.2010.11.013).

## ACKNOWLEDGMENTS

The authors would like to thank Nir Hacohen, Antonio Iavarone, Daphne Koller, Liz Miller, Itsik Pe'er, Suzanne Pfeffer, Neal Rosen, and Olga Troyanskaya for valuable comments. This research was supported by the National Institutes of Health Roadmap Initiative, NIH Director's New Innovator Award Program through grant number 1-DP2-OD002414-01, and National Centers for Biomedical Computing Grant 1U54CA121852-01A1. D.P. holds a Career Award at the Scientific Interface from the Burroughs Wellcome Fund and Packard Fellowship for Science and Engineering.

Received: May 13, 2010

Revised: August 31, 2010

Accepted: October 22, 2010

Published online: December 2, 2010

## REFERENCES

- Adler, A.S., Lin, M., Horlings, H., Nuyten, D.S., van de Vijver, M.J., and Chang, H.Y. (2006). Genetic regulators of large-scale transcriptional signatures in cancer. *Nat. Genet.* *38*, 421–430.
- Beroukhi, R., Getz, G., Nghiemphu, L., Barretina, J., Hsueh, T., Linhart, D., Vivanco, I., Lee, J.C., Huang, J.H., Alexander, S., et al. (2007). Assessing the significance of chromosomal aberrations in cancer: methodology and application to glioma. *Proc. Natl. Acad. Sci. USA* *104*, 20007–20012.

- Beroukhi, R., Brunet, J.-P., Di Napoli, A., Mertz, K.D., Seeley, A., Pires, M.M., Linhart, D., Worrell, R.A., Moch, H., Rubin, M.A., et al. (2009). Patterns of gene expression and copy-number alterations in von-hippel lindau disease-associated and sporadic clear cell carcinoma of the kidney. *Cancer Res.* *69*, 4674–4681.
- Beroukhi, R., Mermel, C.H., Porter, D., Wei, G., Raychaudhuri, S., Donovan, J., Barretina, J., Boehm, J.S., Dobson, J., Urashima, M., et al. (2010). The landscape of somatic copy-number alteration across human cancers. *Nature* *463*, 899–905.
- Bric, A., Miething, C., Bialucha, C.U., Scoppo, C., Zender, L., Krasnitz, A., Xuan, Z., Zuber, J., Wigler, M., Hicks, J., et al. (2009). Functional identification of tumor-suppressor genes through an in vivo RNA interference screen in a mouse lymphoma model. *Cancer Cell* *16*, 324–335.
- Carro, M.S., Lim, W.K., Alvarez, M.J., Bollo, R.J., Zhao, X., Snyder, E.Y., Sulman, E.P., Anne, S.L., Doetsch, F., Colman, H., et al. (2010). The transcriptional network for mesenchymal transformation of brain tumours. *Nature* *463*, 318–325.
- Chiaverini, C., Beuret, L., Flori, E., Busca, R., Abbe, P., Bille, K., Bahadoran, P., Ortonne, J.-P., Bertolotto, C., and Ballotti, R. (2008). Microphthalmia-associated transcription factor regulates RAB27A gene expression and controls melanosome transport. *J. Biol. Chem.* *283*, 12635–12642.
- Chin, L., Garraway, L.A., and Fisher, D.E. (2006). Malignant melanoma: genetics and therapeutics in the genomic era. *Genes Dev.* *20*, 2149–2182.
- Du, J., Widlund, H.R., Horstmann, M.A., Ramaswamy, S., Ross, K., Huber, W.E., Nishimura, E.K., Golub, T.R., and Fisher, D.E. (2004). Critical role of CDK2 for melanoma growth linked to its melanocyte-specific transcriptional regulation by MITF. *Cancer Cell* *6*, 565–576.
- Fischer, T., Stone, R.M., Deangelo, D.J., Galinsky, I., Estey, E., Lanza, C., Fox, E., Ehninger, G., Feldman, E.J., Schiller, G.J., et al. (2010). Phase IIB trial of oral Midostaurin (PKC412), the FMS-like tyrosine kinase 3 receptor (FLT3) and multi-targeted kinase inhibitor, in patients with acute myeloid leukemia and high-risk myelodysplastic syndrome with either wild-type or mutated FLT3. *J. Clin. Oncol.* *28*, 4339–4345.
- Friedman, N., Linal, M., Nachman, I., and Pe'er, D. (2000). Using Bayesian networks to analyze expression data. *J. Comput. Biol.* *7*, 601–620.
- Garraway, L.A., Widlund, H.R., Rubin, M.A., Getz, G., Berger, A.J., Ramaswamy, S., Beroukhi, R., Milner, D.A., Granter, S.R., Du, J., et al. (2005). Integrative genomic analyses identify MITF as a lineage survival oncogene amplified in malignant melanoma. *Nature* *436*, 117–122.
- Golub, T.R., Slonim, D.K., Tamayo, P., Huard, C., Gaasenbeek, M., Mesirov, J.P., Coller, H., Loh, M.L., Downing, J.R., Caligiuri, M.A., et al. (1999). Molecular classification of cancer: class discovery and class prediction by gene expression monitoring. *Science* *286*, 531–537.
- Hoek, K.S., Eichhoff, O.M., Schlegel, N.C., Döbbling, U., Kobert, N., Schaerer, L., Hemmi, S., and Dummer, R. (2008a). In vivo switching of human melanoma cells between proliferative and invasive states. *Cancer Res.* *68*, 650–656.
- Hoek, K.S., Schlegel, N.C., Eichhoff, O.M., Widmer, D.S., Praetorius, C., Einarsson, S.O., Valgeirsdottir, S., Bergsteinsdottir, K., Schepsky, A., Dummer, R., and Steingrimsson, E. (2008b). Novel MITF targets identified using a two-step DNA microarray strategy. *Pigment Cell Melanoma Res* *21*, 665–676.
- Hoek, K.S., Schlegel, N.C., Brafford, P., Sucker, A., Ugurel, S., Kumar, R., Weber, B.L., Nathanson, K.L., Phillips, D.J., Herlyn, M., et al. (2006). Metastatic potential of melanomas defined by specific gene expression profiles with no BRAF signature. *Pigment Cell Res.* *19*, 290–302.
- Itoh, T., Satoh, M., Kanno, E., and Fukuda, M. (2006). Screening for target Rabs of TBC (Tre-2/Bub2/Cdc16) domain-containing proteins based on their Rab-binding activity. *Genes Cells* *11*, 1023–1037.
- Johansson, P., Pavey, S., and Hayward, N. (2007). Confirmation of a BRAF mutation-associated gene expression signature in melanoma. *Pigment Cell Res.* *20*, 216–221.
- Jordens, I., Westbroek, W., Marsman, M., Rocha, N., Mommaas, M., Huizing, M., Lambert, J., Naeyaert, J.M., and Neeffjes, J. (2006). Rab7 and Rab27a control two motor protein activities involved in melanosomal transport. *Pigment Cell Res.* *19*, 412–423.
- Lee, S.-I., Pe'er, D., Dudley, A.M., Church, G.M., and Koller, D. (2006). Identifying regulatory mechanisms using individual variation reveals key role for chromatin modification. *Proc. Natl. Acad. Sci. USA* *103*, 14062–14067.
- Levy, C., Khaled, M., and Fisher, D.E. (2006). MITF: master regulator of melanocyte development and melanoma oncogene. *Trends Mol. Med.* *12*, 406–414.
- Lin, W.M., Baker, A.C., Beroukhi, R., Winckler, W., Feng, W., Marmion, J.M., Laine, E., Greulich, H., Tseng, H., Gates, C., et al. (2008). Modeling genomic diversity and tumor dependency in malignant melanoma. *Cancer Res.* *68*, 664–673.
- Pearl, J. (2000). *Causality: models, reasoning, and inference* (Cambridge, U.K.; New York: Cambridge University Press).
- Pinkel, D., Seagraves, R., Sudar, D., Clark, S., Poole, I., Kowbel, D., Collins, C., Kuo, W.-L., Chen, C., Zhai, Y., et al. (1998). High resolution analysis of DNA copy number variation using comparative genomic hybridization to microarrays. *Nat. Genet.* *20*, 207–211.
- Pleasant, E.D., Cheetham, R.K., Stephens, P.J., McBride, D.J., Humphray, S.J., Greenman, C.D., Varela, I., Lin, M.-L., Ordóñez, G.R., Bignell, G.R., et al. (2010). A comprehensive catalogue of somatic mutations from a human cancer genome. *Nature* *463*, 191–196.
- Pratilas, C.A., Taylor, B.S., Ye, Q., Viale, A., Sander, C., Solit, D.B., and Rosen, N. (2009). (V600E)BRAF is associated with disabled feedback inhibition of RAF-MEK signaling and elevated transcriptional output of the pathway. *Proc. Natl. Acad. Sci. USA* *106*, 4519–4524.
- Sanchez-Garcia, F., Akavia, U.D., Mozes, E., and Pe'er, D. (2010). JISTIC: identification of significant targets in cancer. *BMC Bioinformatics* *11*, 189.
- Sati, D.P., Olson, D.J., van der Vlag, J., Hamer, K.M., Lambrechts, C., Masselink, H., Gunster, M.J., Sewalt, R.G., van Driel, R., and Otte, A.P. (1997). Interference with the expression of a novel human polycomb protein, hPc2, results in cellular transformation and apoptosis. *Mol. Cell. Biol.* *17*, 6076–6086.
- Scott, K.L., Kabbarah, O., Liang, M.-C., Ivanova, E., Anagnostou, V., Wu, J., Dhakal, S., Wu, M., Chen, S., Feinberg, T., et al. (2009). GOLPH3 modulates mTOR signalling and rapamycin sensitivity in cancer. *Nature* *459*, 1085–1090.
- Segal, E., Shapira, M., Regev, A., Pe'er, D., Botstein, D., Koller, D., and Friedman, N. (2003). Module networks: identifying regulatory modules and their condition-specific regulators from gene expression data. *Nat. Genet.* *34*, 166–176.
- Segal, E., Friedman, N., Koller, D., and Regev, A. (2004). A module map showing conditional activity of expression modules in cancer. *Nat. Genet.* *36*, 1090–1098.
- Steingrimsson, E., Copeland, N.G., and Jenkins, N.A. (2004). Melanocytes and the microphthalmia transcription factor network. *Annu. Rev. Genet.* *38*, 365–411.
- Stratton, M.R., Campbell, P.J., and Futreal, P.A. (2009). The cancer genome. *Nature* *458*, 719–724.
- Subramanian, A., Tamayo, P., Mootha, V.K., Mukherjee, S., Ebert, B.L., Gillette, M.A., Paulovich, A., Pomeroy, S.L., Golub, T.R., Lander, E.S., and Mesirov, J.P. (2005). Gene set enrichment analysis: a knowledge-based approach for interpreting genome-wide expression profiles. *Proc. Natl. Acad. Sci. USA* *102*, 15545–15550.
- Taub, N., Teis, D., Ebner, H.L., Hess, M.W., and Huber, L.A. (2007). Late endosomal traffic of the epidermal growth factor receptor ensures spatial and temporal fidelity of mitogen-activated protein kinase signaling. *Mol. Biol. Cell* *18*, 4698–4710.
- Turner, N., Lambros, M.B., Horlings, H.M., Pearson, A., Sharpe, R., Natrajan, R., Geyer, F.C., van Kouwenhove, M., Kreike, B., Mackay, A., et al. (2010). Integrative molecular profiling of triple negative breast cancers identifies amplicon drivers and potential therapeutic targets. *Oncogene* *29*, 2013–2023.

- Vallabhapurapu, S., Matsuzawa, A., Zhang, W., Tseng, P.-H., Keats, J.J., Wang, H., Vignali, D.A.A., Bergsagel, P.L., and Karin, M. (2008). Nonredundant and complementary functions of TRAF2 and TRAF3 in a ubiquitination cascade that activates NIK-dependent alternative NF-kappaB signaling. *Nat. Immunol.* *9*, 1364–1370.
- Wang, K., Saito, M., Bisikirska, B.C., Alvarez, M.J., Lim, W.K., Rajbhandari, P., Shen, Q., Nemenman, I., Basso, K., Margolin, A.A., et al. (2009a). Genome-wide identification of post-translational modulators of transcription factor activity in human B cells. *Nat. Biotechnol.* *27*, 829–839.
- Wang, L., Cao, X.X., Chen, Q., Zhu, T.F., Zhu, H.G., and Zheng, L. (2009b). DIXDC1 targets p21 and cyclin D1 via PI3K pathway activation to promote colon cancer cell proliferation. *Cancer Sci.* *100*, 1801–1808.
- Wellbrock, C., Rana, S., Paterson, H., Pickersgil, H., Brummelkamp, T., and Marais, R. (2008). Oncogenic BRAF regulates melanoma proliferation through the lineage specific factor MITF. *PLoS ONE* *3*, e2734.
- Ying, H., Zheng, H., Scott, K., Wiedemeyer, R., Yan, H., Lim, C., Huang, J., Dhakal, S., Ivanova, E., Xiao, Y., et al. (2010). Mig-6 controls EGFR trafficking and suppresses gliomagenesis. *Proc. Natl. Acad. Sci. USA* *107*, 6912–6917.
- Zender, L., Xue, W., Zuber, J., Semighini, C.P., Krasnitz, A., Ma, B., Zender, P., Kubicka, S., Luk, J.M., Schirmacher, P., et al. (2008). An oncogenomics-based in vivo RNAi screen identifies tumor suppressors in liver cancer. *Cell* *135*, 852–864.